

# The conformational landscape of 5-methoxytryptamine studied by rotationally resolved fluorescence spectroscopy and resonant ionization spectroscopy

Thi Bao Chau Vu,<sup>a</sup> Ivo Kalkman,<sup>b</sup> W. Leo Meerts,<sup>b</sup> Christian Brand,<sup>a</sup> Yuriy N. Svartsov,<sup>a</sup> Sascha Wiedemann,<sup>a</sup> Rainer Weinkauff<sup>a</sup> and Michael Schmitt\*<sup>a</sup>

Received 4th November 2008, Accepted 26th January 2009

First published as an Advance Article on the web 16th February 2009

DOI: 10.1039/b819469f

Rotationally resolved electronic spectra of three different conformers of 5-methoxytryptamine were recorded in a molecular beam. 5-Methoxy substitution reduces the number of observed conformers to three compared to seven that have been reported for tryptamine. Quantum chemical calculations indicate that *anti*-rotamers of the methoxy-group are more stable relative to the *syn*-forms. Two *gauche* structures (Gpy(in) and Gph(in)) of the ethylamino group with respect to the indole chromophore were found to be less stable than the other seven. The lowest electronically excited state has been identified as the <sup>1</sup>L<sub>b</sub> one for all observed conformers which was confirmed by quantum-chemical calculations. Based on the comparison of rotational constants obtained from fits using evolutionary algorithms with those from calculations, the three observed conformers were determined to be the Gpy(up), Gph(up), Gpy(out) ethylamino side-chain conformations.

## 1. Introduction

Ethylamino substituted indole derivatives like tryptamine (2-(1H-indol-3-yl)ethanamine), serotonin (3-(2-aminoethyl)-1H-indol-5-ol), melatonin (N-[2-(5-methoxy-1H-indol-3-yl)ethyl]ethanamide) and mexamin (2-(5-methoxy-1H-indol-3-yl)ethanamine) have found considerable interest due to their effect as neurotransmitters, radiation protecting agents or sedatives. The present publication presents an investigation of the conformational isomers of mexamin (also called 5-methoxytryptamine) using a combination of low resolution ionization spectroscopy, rotationally resolved electronic spectroscopy, and *ab initio* theory.

The crystal structure of 5-methoxytryptamine has been determined to be monoclinic by X-ray crystallography. The ethylamino side-chain was found to be bent into the *gauche* or synclinal conformation.<sup>1</sup> Bayari and Ide presented a vibrational analysis of 5-methoxytryptamine in KBr using FTIR spectroscopy. Additionally they took the X-ray diffraction pattern of 5-methoxytryptamine and determined the preferential conformation in the crystal to be in *anti* position.<sup>2</sup>

Tryptamine has become a model system, for which the conformational landscape has been studied intensively over a long period.<sup>3–10</sup> The rotationally resolved electronic spectrum of tryptamine in a molecular beam has been reported several times in the past few years at increasingly good resolutions,

thus unravelling more details of its conformational landscape.<sup>6–10</sup> Caminati determined the rotational constants of the A and B conformers of tryptamine in the electronic ground state using microwave spectroscopy and made an assignment to the structures based on *ab initio* calculations.<sup>11</sup> Dian *et al.* determined the energy thresholds between the different conformers of tryptamine using stimulated emission pumping-hole filling and stimulated emission pumping-induced population transfer spectroscopy.<sup>12,13</sup>

Improved theoretical methods for the description of electronically excited states facilitate the computation of various properties like structure, adiabatic excitation energies, permanent and transition dipole moments, *etc.* with nearly spectroscopic accuracy.<sup>14</sup>

Much less structural information can be found for serotonin and melatonin. LeGreve *et al.* performed laser induced fluorescence (LIF), resonance enhanced multiphoton ionization (REMPI), UV–UV double resonance (UV–UV DR) and resonant ion-dip infrared (RIDIR) spectroscopy on serotonin and identified 8 different conformers.<sup>15</sup> For melatonin Florio *et al.*<sup>16</sup> found and assigned five different conformers on the basis of IR–UV double resonance spectroscopy.

It has been found that small changes in the system like water attachment to flexible molecules can considerably change the energetics of the conformational landscape.<sup>9</sup> In this paper we address the question how a methoxy substitution in position 5 of the indole ring changes the conformational landscape of tryptamine. Since the distance between the methoxy and the ethylamino groups is considerably large, one would expect a very weak direct interaction and hence a negligible effect on conformational preferences. We will show in this paper that this is not the case.

<sup>a</sup>Heinrich-Heine-Universität, Institut für Physikalische Chemie I, D-40225 Düsseldorf, Germany. E-mail: mschmitt@uni-duesseldorf.de

<sup>b</sup>Molecular and Biophysics Group, Institute for Molecules and Materials, Radboud University Nijmegen, NL-6500 GL Nijmegen, The Netherlands

## 2. Techniques

### 2.1 Experimental procedures

5-Methoxytryptamine (98%) was purchased from Sigma Aldrich and used without further purification. The experimental setup for the rotationally resolved laser induced fluorescence is described in detail elsewhere.<sup>17</sup> Briefly, the laser system consists of a single frequency ring dye laser (Coherent 899-21) operated with Kiton Red, pumped with 7 W of the 515 nm line of a frequency doubled cw Nd:YAG laser. The dye laser output is coupled into an external folded ring cavity (Spectra Physics Wavetrain) for second harmonic generation. The resulting output power was constant at about 15 mW during each experiment. The molecular beam is formed by co-expanding 5-methoxytryptamine, heated to 200 °C, and 200 mbar of argon through a 200  $\mu\text{m}$  nozzle into the vacuum. The molecular beam machine consists of three differentially pumped vacuum chambers that are linearly connected by skimmers (1 and 3 mm, respectively) in order to reduce the Doppler width. The resulting resolution is 25 MHz in this setup (FWHM). In the third chamber, 360 mm downstream of the nozzle, the molecular beam crosses the laser beam at a right angle. The imaging optics setup consists of a concave mirror and two plano-convex lenses to collect the resulting fluorescence onto a photomultiplier tube, which is mounted perpendicular to the plane defined by the laser and molecular beam. The signal output is then discriminated and digitized by a photon counter and transmitted to a PC for data recording and processing. The relative frequency is determined with a quasi-confocal Fabry–Perot interferometer. The absolute frequency is obtained by comparing the recorded iodine absorption spectrum with tabulated lines.<sup>18</sup>

The experimental setup for the low-resolution REMPI experiment is described in detail elsewhere.<sup>19</sup> In short, the sample molecules are heated to 110 °C to form a suitable partial pressure in a pulsed valve (General Valve) flooded with 4 bar Ar carrier gas. The pulsed supersonic beam is pulsed into a first vacuum chamber, then skimmed after 30 mm and finally ionized *ca* 200 mm downstream the valve in a second vacuum chamber. Ions are accelerated in a two-stage ion source and mass detected in a linear time-of-flight mass spectrometer. For REMPI spectroscopy the gated ion signal is recorded in dependence on the laser wavelength. The excitation light was provided by a frequency-doubled conventional Nd:YAG laser-pumped dye laser (7 ns pulse width). The laser was used without lens to avoid saturation in the excitation processes (100  $\mu\text{J pulse}^{-1}$ , 4 mm<sup>2</sup> laser beam size).

### 2.2 Computational methods

**2.2.1 Quantum mechanical calculations.** Structure optimizations were performed employing the valence triple zeta basis set with polarization functions (d,p) from the TURBOMOLE library.<sup>20,21</sup> The equilibrium geometries of the electronic ground states were optimized at the level of density functional theory using the B3-LYP-D functional<sup>22</sup> corrected for long range dispersion interactions.<sup>23,24</sup> These dispersion interactions account for interactions of the ethylamino side-chain with the  $\pi$ -system of the chromophore, present in

the four *gauche* conformers. Zero-point energy correction was accounted for through vibrational harmonic frequencies which have been calculated through analytical second derivatives of the B3-LYP energies using the aoforce module<sup>25,26</sup> implemented in Turbomole Version 5.9.

**2.2.2 The evolutionary algorithms for fitting of the rovibronic spectra.** The rotationally resolved electronic spectra were fit to a simple asymmetric rotor Hamiltonian using the derandomized-ES DR2 algorithm, an evolutionary strategy developed by Ostenmeier *et al.*<sup>27</sup> which has been shown recently to be a very good alternative for the automated assignment of rotationally resolved electronic spectra of molecules which are highly congested<sup>28</sup> compared to the genetic algorithm based fits we have employed so far.<sup>29–32</sup> Both strategies—the derandomized-ES DR2 algorithm and the genetic algorithm—belong to the category of global optimizers whose concepts are copied from evolutionary concepts in nature.

Their main difference lies in the fact that while the genetic algorithm tries to find a solution in parameter space by randomly combining information from a set of trial solutions, the steps in the DR2 algorithm are influenced by their history. In a first step, some trial solutions are generated from a random distribution around some starting point, each consisting of the complete parameter set necessary to describe the spectrum, and the quality of each solution is analyzed using a fitness function. If one of the solutions, obtained in the combination of information is better than the original one, this solution is selected and used to compute the next parent generation, which then serves as the starting point for an iteration of this cycle. In the calculation of the parent for the next generation the DR2 algorithm makes use of the correlation matrix for successive changes in the parents (mutations). This means that whenever for some parameter a parent has evolved in the same direction for several generations, so that their correlation in this parameter is positive, the most likely solution is assumed to be further in that direction and the next parameter mutation step will be larger. Correspondingly, two *anti*-correlated mutations will lead to a smaller mutation size.

## 3. Results

### 3.1 Computational results

The structures of fourteen different conformers of 5-methoxytryptamine have been optimized at the B3-LYP-D/TZVP level of theory using dispersion corrected functionals from Grimme.<sup>23,24</sup> Using the notation of Carney *et al.*, these are labelled as Gpy(out), Gpy(up), Gph(out), Gph(up), Anti(py), Anti(ph), and Anti(up) conformers describing the orientation of the ethylamino side-chain with respect to the indole ring (*gauche* on the pyrrole side, *gauche* on the phenyl side or *anti*), and the orientation of the amino lone pair (pointing up, out, to the phenyl side or to the pyrrole side). Like in tryptamine itself, the (in) conformers of Gph and Gpy with the lone pair pointing to the aromatic ring are of much higher energy and will not be considered here. The number of possible conformers compared to tryptamine is doubled in

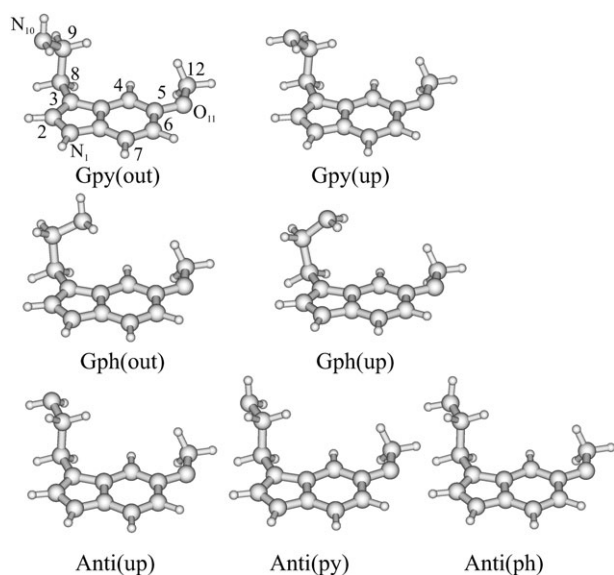


**Fig. 1** DFT-D optimized *anti(OMe)* structures of seven conformers of 5-methoxytryptamine. The Gpy(out) structure contains the atomic numbering used in this publication.

5-methoxytryptamine, because the methoxy group in 5-position can be oriented in the direction of the ethylamino side-chain (*anti(OMe)*) or opposing the side-chain (*syn(OMe)*). All *syn(OMe)* conformers are at least 3.5 kJ/mole higher in energy than their *anti(OMe)* counterparts.

Fig. 1 shows the seven optimized *anti(OMe)* structures, Table 1 gives the rotational constants, inertial defects and relative energies of all rotamers (*syn(OMe)* and *anti(OMe)*) at the B3-LYP-D/TZVP level of theory. A complete analysis and comparison of the methoxytryptamine and serotonin conformational space is performed and will be published soon.<sup>33</sup>

While density functional theory does not account properly for the dispersive interactions between the ethylamino side-chain and the  $\pi$ -system of the chromophore and thus underestimates the energy differences of the *gauche* and the *anti* conformers, Møller–Plesset perturbation theory on second order (MP2) has been shown in related molecules like

tryptamine<sup>12,14,34</sup> and serotonin<sup>15</sup> to give the correct energy ordering of the conformers. Nevertheless, MP2 calculations are computationally very expensive compared to DFT methods. We therefore decided to use the dispersion corrected Becke-3LYP-D functional which has been shown to correctly account for dispersive van der Waals interactions.<sup>23</sup>

In contrast to the tryptamine case, where the Gpy(out) conformer was found to be the most stable one, we predict for 5-methoxytryptamine the Gph(out) conformer to be the most stable one. This agrees with MP2 calculations of LeGreve *et al.*<sup>15</sup> on 5-hydroxytryptamine conformers which find the Gph(out) conformer as most stable one, followed by the Gpy(out) conformer. DFT calculations, performed in the same work put the energy ordering as in the tryptamine case. This (incorrect) ordering was also found in a DFT study by van Mourik *et al.*<sup>35</sup> and shows the necessity of considering the dispersion forces correctly.

The quite large stabilization of the *gauche* conformers relative to the *anti* conformers is a consequence of the consideration of the long range dispersions and shows the advantage of the dispersion corrected density functionals over the standard ones, for the description of the conformational stabilities.

The vibrational frequencies of the Gpy(out) conformer in the range of the large amplitude torsional motions have been calculated for the electronic ground state using analytical second derivatives of the RIMP2 energy using the Aoforce module from the Turbomole package. The lowest frequency at 39.2 cm<sup>-1</sup> can be assigned to the torsional motion  $\tau_1$  of the C3C8 bond. The energetically following vibration at 68.2 cm<sup>-1</sup> is a bending motion of the ethylamino side-chain relative to the indole ring ( $\beta_1$ ) with an admixture of methoxy bending. The vibration at 96.2 cm<sup>-1</sup> is a combined methoxy and ethylamino bending mode. The torsional motion  $\tau_2$  about the C8C9 bond is found at 124.7 cm<sup>-1</sup>. Further bands at 153.2 and 267.4 cm<sup>-1</sup> can be assigned to combinations of bending and torsional motions mainly localized in the methoxy group and inversion motion at the indolic NH group. Out-of-plane vibrations of the indole chromophore at 169.9 and 212.1 cm<sup>-1</sup> are assigned to the 10b and 10a vibrations in

**Table 1** DFT-D (B3-LYP-D/TZVP) calculated rotational constants (*A*, *B*, *C*) the inertial defects ( $\Delta I$ ) and relative energies ( $\Delta E$ ) of fourteen conformers of 5-methoxytryptamine in their electronic ground state. Stabilization energies contain zero-point corrections using the B3-LYP/TZVP harmonic frequencies

Anti(OMe)							
Aoforce	Gpy(out)	Gpy(up)	Gph(out)	Gph(up)	Anti(py)	Anti(ph)	Anti(up)
<i>A</i> /MHz	979	965	908	916	850	848	847
<i>B</i> /MHz	512	517	585	572	525	529	527
<i>C</i> /MHz	367	368	380	380	336	337	336
$\Delta I/\text{amu } \text{Å}^2$	-126.2	-127.9	-90.5	-105.3	-53.1	-51.7	-51.5
$\Delta E/\text{cm}^{-1}$	93.4	89.0	0	203.9	554.1	501.1	765.8
Syn(OMe)							
<i>Anti</i>	Gpy(out)	Gpy(up)	Gph(out)	Gph(up)	Anti(py)	Anti(ph)	Anti(up)
<i>A</i> /MHz	1155	1141	1056	1064	990	991	989
<i>B</i> /MHz	443	445	496	491	448	449	447
<i>C</i> /MHz	348	349	358	360	318	318	318
$\Delta I/\text{amu } \text{Å}^2$	-126.1	-130.5	-85.8	-100.4	-49.3	-46.3	-52.4
$\Delta E/\text{cm}^{-1}$	408.9	420.6	509.8	529.7	829.1	859.4	458.1

**Table 2** Vibrational frequencies below 300 cm<sup>-1</sup> of the seven most stable Anti(OMe) conformers of 5-methoxytryptamine

Mode	Gpy(out)	Gpy(up)	Gph(out)	Gph(up)	Anti(py)	Anti(ph)	Anti(up)
$\tau_1$	39.2	36.9	54.4	42.0	48.5	49.0	48.8
$\beta_1$	68.2	67.0	80.5	73.6	66.7	66.4	66.9
$\beta_1$	96.2	95.0	92.6	86.7	92.6	90.4	92.7
$\tau_2$	124.7	119.1	126.8	124.2	98.3	98.3	97.9
$N_{inv.}$	153.2	153.2	152.7	152.2	153.3	153.2	153.4
10b	169.9	168.8	177.1	175.6	175.5	175.6	176.3
10a	212.1	209.8	220.3	209.1	202.9	201.0	201.1
$N_{inv.}$	267.4	266.7	262.8	266.6	239.0	239.6	261.3

the classification scheme of Varsanyi.<sup>36</sup> Most of the modes strongly couple methoxy and ethylamino torsional motions, so that no unequivocal description of the mode as in the case of tryptamine can be given. The approximate descriptions of the modes given in Table 2 have been taken from ref. 37. Table 2 compares the vibrational frequencies below 300 cm<sup>-1</sup> of the seven Anti(OMe) conformers.

### 3.2 Low resolution R2PI spectra of 5-methoxytryptamine

Low-resolution R2PI spectra were recorded to obtain overview spectra and to identify spectral contributions of clusters with water. Fig. 2 shows the R2PI spectrum of 5-methoxytryptamine in the range between 32 450 and 32 950 cm<sup>-1</sup>. Trace (a) shows the R2PI spectrum at  $m/z = 190$  Da (the methoxytryptamine mass) using the methoxytryptamine sample as obtained. In a next step, to avoid contamination by methoxytryptamine–water cluster peaks, the sample was thoroughly dried. All peaks red to 32 700 and blue to 32 900 practically vanished as shown in trace (b). Trace (c) finally shows the R2PI spectrum with addition of 18 mbar of water to the Ar carrier gas, recorded at the mass channel of methoxytryptamine + water

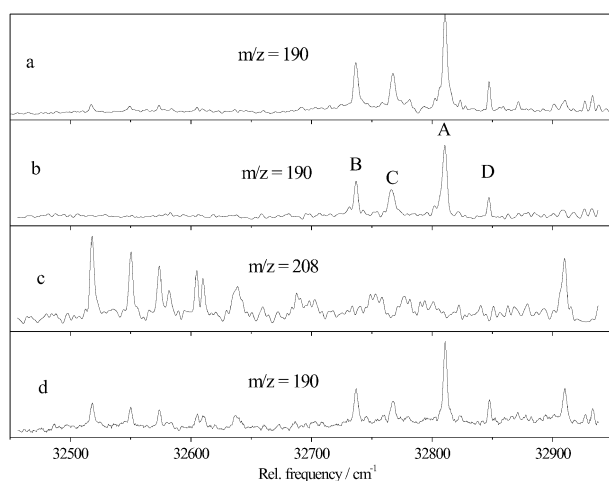


**Fig. 2** (a) R2PI spectrum taken on the mass channel of 5-methoxytryptamine ( $m/z = 190$  Da). (b) R2PI spectrum taken on the mass channel of 5-methoxytryptamine ( $m/z = 190$  Da) after thorough drying of the sample. (c) R2PI spectrum taken on the mass channel of 5-methoxytryptamine(H<sub>2</sub>O)<sub>1</sub> ( $m/z = 208$  Da) after addition of 18 mbar of water to the Ar carrier gas. (d) Conditions like in (c), but spectrum taken at the mass channel 190 Da.

( $m/z = 208$  Da). None of these bands could be detected on higher mass channels from larger water clusters. Thus, we tentatively assign all bands shown in trace (c) to the 5-methoxytryptamine(H<sub>2</sub>O)<sub>1</sub> cluster. The spectrum is governed by long progressions in low frequency modes and differs considerably from the R2PI spectra of tryptamine(H<sub>2</sub>O)<sub>1</sub><sup>38</sup> and indole(H<sub>2</sub>O)<sub>1</sub>.<sup>39</sup>

Four different bands can be assigned on the basis of the R2PI spectrum of Fig. 2b to belong to the 5-methoxytryptamine monomer. They are labelled by A–D according to their intensities. Band D at 32 844.73 cm<sup>-1</sup> was too weak to obtain a rotationally resolved spectrum with a sufficiently good signal/noise ratio for assignment. Anyhow, from the frequency of 36.6 cm<sup>-1</sup> relative to the origin of the A conformer, it is probable that this band represents a vibrational mode of the A conformer due to the torsional motion of the ethylamino side-chain about the C8C9 bond, *cf.* Table 2. Nevertheless, we cannot exclude completely a fourth conformer for being responsible for this band. Rotationally resolved spectra of the three bands A–C will be presented in section 3.

### 3.3 High resolution spectra of conformers of 5-methoxytryptamine

Fig. 3 shows the rotationally resolved spectrum of the conformer A of 5-methoxytryptamine along with a simulation,

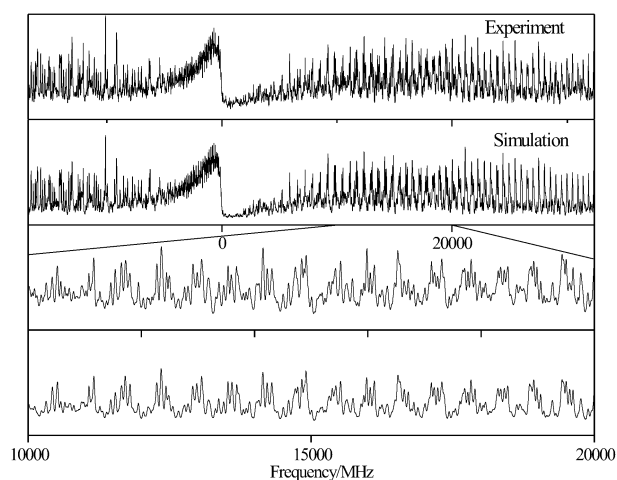


**Fig. 3** Rotationally resolved electronic spectrum of the A band of 5-methoxytryptamine. The second trace shows the simulation using the best parameters from Table 3. The lowest traces show zoomed-in parts of the experimental spectrum and the simulation.

**Table 3** Molecular constants of the three conformers of 5-methoxytryptamine obtained from ES-DR2 fits to the experimental spectra. The changes of the ground state rotational constants  $A''$ ,  $B''$ , and  $C''$  upon electronic excitation are defined as:  $\Delta A = A' - A''$  etc., where  $A'$  are the rotational constants in the electronically excited state.  $\Delta I$  is the inertial defect in  $\text{amu } \text{\AA}^2$  and  $\Delta \Delta I$  its change upon electronic excitation

Exp.	Conf. A	Conf. B	Conf. C
$A''/\text{MHz}$	990.88(12)	914.40(11)	976.85(12)
$B''/\text{MHz}$	500.27(9)	569.18(8)	504.49(9)
$C''/\text{MHz}$	361.57(9)	376.74(8)	362.65(9)
$\Delta I/\text{amu } \text{\AA}^2$	-122.49	-99.14	-125.41
$\theta/^\circ$	78(6)	77(6)	80(6)
$\phi_2/^\circ$	40(6)	46(6)	45(6)
$\mu_a$	57	46	49
$\mu_b$	39	49	48
$\mu_c$	4	5	3
$\tau/\text{ns}$	11.2(24)	10.2(20)	—
$\nu_0/\text{cm}^{-1}$	32 808.13(2)	32 733.82(2)	32 763.49(2)
$\Delta A/\text{MHz}$	-5.44(3)	-7.45(3)	-5.09(3)
$\Delta B/\text{MHz}$	-3.22(4)	-2.38(4)	-3.06(4)
$\Delta C/\text{MHz}$	-2.49(4)	-2.23(4)	-2.18(4)
$\Delta \Delta I/\text{amu } \text{\AA}^2$	-122.14	-99.40	-125.80

using the best parameters from the derandomized-ES DR2 fit given in Table 3. The uncertainties of the parameters are given in parentheses and are obtained as standard deviations by performing a quantum number assigned fit. In this fit those transitions obtained from the derandomized-ES DR2 fit are included that would be used in a typical manual assignment of the spectra, that is transitions with intensity larger than 5% of the maximum intensity and with rotational quantum numbers up to  $J = 10$ .

Even what appears to be single rovibronic lines in the  $P$  or  $R$  branch of the simulated spectrum are superpositions of some ten rovibronic transitions. This fact highlights the necessity for an automated fitting technique like the evolutionary strategies employed here. Band A at  $32808.13 \text{ cm}^{-1}$  is predominantly an  $ab$  hybrid type transition, with 57%  $a$ -type, 39%  $b$ -type, and 4%  $c$ -type character. The lifetime is determined to be around 10 ns from a Lorentz contribution of 14 MHz to the full Voigt

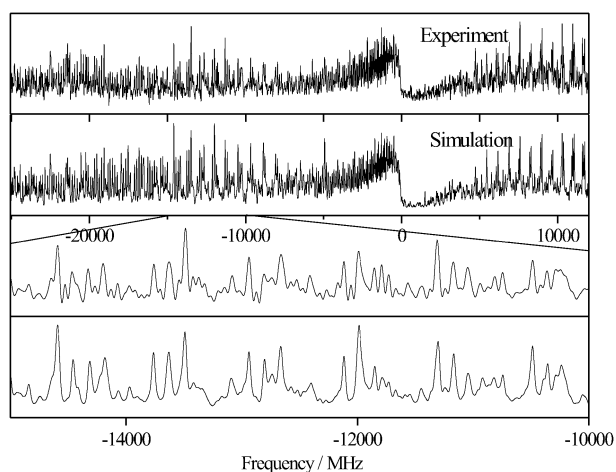


**Fig. 4** Rotationally resolved electronic spectrum of band B of 5-methoxytryptamine. The second trace shows the simulation using the best parameters from Table 3. The lowest traces show zoomed-in parts of the experimental spectrum and the simulation.

line width. From the rotational constants an inertial defect of  $-122.5 \text{ amu } \text{\AA}^2$  for the ground state and of  $-122.1 \text{ amu } \text{\AA}^2$  for the electronically excited state is calculated.

The high resolution spectrum of the B band of 5-methoxytryptamine at  $32733.8 \text{ cm}^{-1}$  is shown in Fig. 4. Like band A, this transition is predominantly polarized in the  $ab$  plane, with an excited state lifetime of approximately 10 ns. The inertial defect in the ground state is  $-99.14 \text{ amu } \text{\AA}^2$  and in the excited state  $-99.40 \text{ amu } \text{\AA}^2$ , considerably smaller than in the A conformer.

Fig. 5 shows the high resolution spectrum of band C at  $32763.5 \text{ cm}^{-1}$ . This band consists of two rovibronic spectra, separated by *ca* 2000 MHz. One of these spectra is unambiguously fitted with the molecular parameters given in Table 3. The spectral features of the other component are too different (*cf.* the lowest trace in Fig. 5, which gives the residue of the experimental and simulated spectrum) to be due to another 5-methoxytryptamine conformer. It consists more or less only of a pronounced  $Q$ -branch structure, with hardly any  $P$  or  $R$  band intensity. The mass spectrum shows a mass of 161 coming up, while scanning over band C. This might be a fragment from 5-methoxytryptamine, formed by thermal decomposition in the source, cleaving a  $\text{CH-NH}_2$  fragment, and leaving 3-methyl-5-methoxyindole. Since the chromophore and its direct surrounding are the same to 5-methoxytryptamine it is not improbable that the absorption takes place spectrally very close.

The density of lines in band C of methoxytryptamine is so high (mainly due to the overlapping second band), that no reliable Lorentzian width can be determined and, consequently, no lifetime is given in Table 3. The inertial defect of band C is  $-125.41 \text{ amu } \text{\AA}^2$  in the ground state and  $-125.80 \text{ amu } \text{\AA}^2$  in the electronically excited state, thus the largest of all three conformers.

The changes of the rotational constants upon electronic excitation of the three conformers are all negative, quite small and similar, in contrast to the changes in tryptamine.<sup>9</sup>

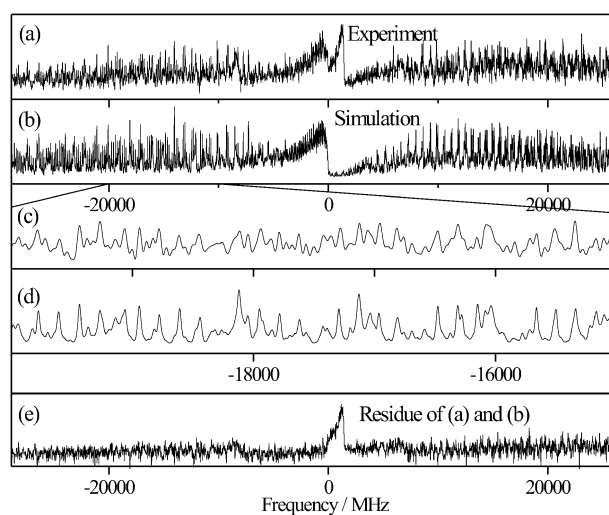


**Fig. 5** Rotationally resolved electronic spectrum of band C of 5-methoxytryptamine. The second trace shows the simulation using the best parameters from Table 3. The next two traces show zoomed-in parts of the experimental spectrum and the simulation. The lowest trace gives the residue of the experimental and the simulated spectrum.

## 4. Discussion

The R2PI spectra of 5-methoxytryptamine show a considerable number of bands, which belong to the clusters with water. Differing from the tryptamine case a number of cluster bands appear. Although the clusters with water are not the central topic of this publication we also tried to record the rotationally resolved spectra of the clusters. Unfortunately, we did not succeed in getting any high resolution spectrum of the clusters of methoxytryptamine with water. This is probably due to the very different expansion conditions in the pulsed R2PI and the continuous LIF experiment. Further work is on the way, to adapt the expansion conditions in the cw experiment in order to be able to record the high resolution spectra of the clusters with water as well.

### 4.1 Assignment of the conformers

The assignment of the three origin bands of 5-methoxytryptamine conformers to the structure only on the basis of their rotational constants is difficult, because the calculated differences within the Gpy, the Gph, and the Anti families are small (*cf.* Table 1), while the distinction between the *syn(OMe)* and *anti(OMe)* structures poses no problems. Table 4 gives the  $\chi^2$  values for the calculated and experimental rotational constants for the four different *Anti(OMe) gauche* conformers.

The assignment for band B, being due to the *Anti(OMe)-Gph(up)* conformer from the  $\chi^2$  value is straightforward. The assignment of structures to bands A and C on the basis of the least squares of the rotational constants only is not so unambiguous, because both Gpy(out) and Gpy(up) structures have small  $\chi^2$  values for the A as well as for band C.

Therefore, in addition to the least squares of the calculated and the experimental rotational constants, we also employed the differences of rotational constants between the conformers under consideration and the inertial defects of the conformers. Table 5 shows the differences of the experimental rotational constants and inertial defect of conformers A and C compared to the difference of the calculated Gpy(out) and Gpy(up) rotational constants and their inertial defect. Since differences of calculated rotational constants show less errors as the absolute numbers, we present the differences of the experimental and calculated rotational constants between A and C in Table 5. The good agreement and the correct sign show that this assignment is right. Note that a reversed assignment would especially lead to switching of the signs.

**Table 4**  $\chi^2$  values  $((A_{\text{exp}} - A_{\text{calc}})^2/\sigma_A^2 + (B_{\text{exp}} - B_{\text{calc}})^2/\sigma_B^2 + (C_{\text{exp}} - C_{\text{calc}})^2/\sigma_C^2)$  obtained from experimental rotational constants ( $A_{\text{exp}}$ ,  $B_{\text{exp}}$ , and  $C_{\text{exp}}$ ) and their standard deviations ( $\sigma_A$ ,  $\sigma_B$ , and  $\sigma_C$ ) from Table 3 for the three different bands A, B and C and calculated rotational constants ( $A_{\text{calc}}$ ,  $B_{\text{calc}}$ , and  $C_{\text{calc}}$ ) from Table 1 for the *Anti(OMe)* conformers of Gpy(out), Gpy(up), Gph(out), and Gph(up)

Conf.	Gpy(out)	Gpy(up)	Gph(out)	Gph(up)
A	30 428	86 171	1 405 272	1 066 519
B	870 580	648 966	44 151	3 115
C	9620	32 606	1 166 582	856 963

**Table 5** Ground state difference of the rotational constants ( $\Delta A'' = A''(\text{conformer A}) - A''(\text{conformer C})$ ;  $\Delta B''$ , and  $\Delta C''$ , respectively) and difference of the inertial defect ( $\Delta\Delta I''$ ) of conformer A and conformer C ( $\Delta\Delta I'' = \Delta I''(\text{conformer A}) - \Delta I''(\text{conformer C})$ ) compared to the respective calculated difference of *gauche* pyrrole out and up obtained from the DFT-D calculations

	<i>Gauche</i> pyrrole	
	Experiment	Calculated
	conf. A – conf. C	out-up
$\Delta A''/\text{MHz}$	14.1	14
$\Delta B''/\text{MHz}$	–4.8	–5
$\Delta C''/\text{MHz}$	–1.1	–1
$\Delta\Delta I''/\text{amu } \text{Å}^2$	3.0	1.69

### 4.2 Determination of the structure parameters

The determination of only three rotational constants for each conformer allows of course only the determination of three geometrical parameters, keeping all others fixed. We performed a fit of angle  $\alpha_1$  (C8C9N10), the dihedral angles  $\text{dih}_2$  (C3C8C9N10), and  $\text{dih}_3$  (C2C3C8C9) (*cf.* Fig. 1 for the atomic numbering) with all other geometry parameters held fixed at the values of the DFT-D optimized structures using the program pKRFit.<sup>40,41</sup> The resulting structural parameters in Table 6 are  $r_0$  parameters, incorporating the effects of zero-point motions. Further investigations with other isotopomers have to be performed to further refine these results.

### 4.3 Orientation of the transition dipole moment

The transition dipole moment (TDM) in all three conformers is located in the *ab* plane, and oriented as shown in Fig. 6 and Table 7. There are two possible orientations of the transition dipole moment (I and II in Fig. 6), since the relative intensities of the rovibronic bands in the experimental spectra depend on the projection of the TDM onto the inertial axes. Comparing this orientation to the results of DFT/MRCI calculations on TDDFT/TZVP optimized structures,<sup>33</sup> and to the orientation of the transition dipole moment in the lowest electronically excited state of tryptamine<sup>5</sup> and 5-methoxyindole<sup>42</sup> it is found that orientation I is observed, which corresponds to that of the  $L_b$  state. Thus, like for tryptamine itself, the lowest electronically excited state is  $L_b$ . The experimental adiabatic excitation energy for the Gph(up) conformers is  $32\,734\text{ cm}^{-1}$ , for Gpy(out)  $32\,808\text{ cm}^{-1}$ , and for Gpy(up)  $32\,763\text{ cm}^{-1}$ .

They are compared in Table 7 to the excitation energies of the respective tryptamine conformers. The relative excitation energies have the same energetic ordering as in tryptamine, thus further confirming the assignment of the absorption features to the geometries of the described conformers.

**Table 6** Fitted geometry parameters of the three 5-methoxytryptamine conformers studied in this work. For the definition of the angles and dihedral angles *cf.* Fig. 1

	$\alpha_1$ C8C9N10	$\text{dih}_2$ C3C8C9N10	$\text{dih}_3$ C2C3C8C9
Gpy(out)	111.08(20)	–65.58(4)	102.23(2)
Gph(up)	112.86(23)	68.85(3)	90.72(1)
Gpy(up)	116.57(22)	–63.38(4)	103.8(2)

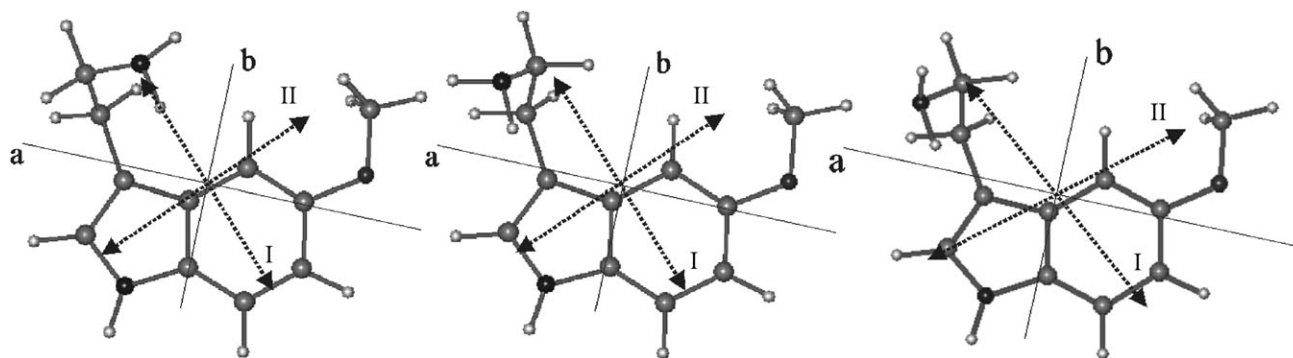


**Fig. 6** Orientation of the transition dipole moment in the inertial frame of the Gph(up), Gpy(up), and Gpy(out) conformers of 5-methoxytryptamine.

**Table 7** Comparison of adiabatic excitation energies and transition dipole moment orientations in tryptamine and 5-methoxytryptamine

(OMe)	Tryptamine				5-Methoxytryptamine			
	$\nu_0$	$\Delta\nu_0$	$\phi$	$\theta$	$\nu_0$	$\Delta\nu_0$	$\phi$	$\theta$
Gph(up)	34 832	0	81	14	32 734	0	77	46
Gpy(up)	34 896	64	72	22	32 763	29	80	46
Gpy(out)	34 916	84	72	14	32 808	74	80	39

## 5. Conclusions

The rotationally resolved electronic spectra of three different conformers of 5-methoxytryptamine were analyzed and assigned to the Gph(up) (band B), the Gpy(out) (band A), and the Gpy(up) (band C) structures. Band D can be tentatively assigned to the torsional motion  $\tau_1$  of the ethylamino side-chain of conformer A. The experimental frequency is  $36.6 \text{ cm}^{-1}$ , the calculated frequency (RIMP2/TZVP) of the Gpy(out) conformer  $39.2 \text{ cm}^{-1}$ . The same vibrational band for the Gph(up) conformer is calculated to be  $42 \text{ cm}^{-1}$  and shows very weakly up in the red wing of band C, while for the Gpy(up) conformer it is calculated to be  $36.9 \text{ cm}^{-1}$ , weakly showing up red to the origin of band A. The origin bands of all three conformers belong to the  ${}^1L_b$  electronic state. Good agreement is found between the experimental rotational constants and those extracted from optimized structures, using dispersion corrected density functionals. These structures closely resemble the experimentally found ones, with an energy ordering of Gph(out) < Gpy(up) < Gpy(out) < Gph(up) < Anti(ph) < Anti(py) < Anti(up). This energetic ordering of conformers is the same that LeGreve *et al.*<sup>15</sup> have found for the similar 5-hydroxytryptamine system, showing the reliability of the dispersion correction for examination of the conformational spaces of this class of molecules. The three most stable structures are in good agreement with the experiment.

In 5-methoxytryptamine only *Anti(OMe)* structures of the methoxy group and *gauche* structures of the ethylamino side-chain are found. Since tryptamine itself has already 7 low-lying thermally populated conformers and the methoxy group in 5-methoxytryptamine adds one more conformational dimension to this, one would expect to observe even more than 7 conformers. Instead, only 3 conformers of 5-methoxytryptamine are found in the experiment. It is improbable that some of the

conformers have much shorter lifetimes which may prevent them from being observed in a highly resolving experiment. Therefore, the reason for the preferential stabilization of the *gauche* conformers in methoxytryptamine must be a changed electrostatic interaction of the ethylamino side-chain with the indole chromophore upon substitution with a methoxy group in 5-position.

## Acknowledgements

This work has been performed in the SFB 663 TP A2 (Schmitt) and A1 (Weinkauff) Universität Düsseldorf and was printed with financial support from the Deutsche Forschungsgemeinschaft. The authors like to thank the National Computer Facilities of the Netherlands Organisation of Scientific Research (NWO) for a grant on the Dutch supercomputing facility SARA. This work was also supported by the Netherlands Organization for Scientific Research and the Deutsche Forschungsgemeinschaft in the framework of the NWO–DFG bilateral programme (SCHM1043/10-1).

## References

- W. G. Quarles, D. H. Templeton and A. Zalkin, *Acta Crystallogr., Sect. B*, 1974, **30**, 95–98.
- S. Bayari and S. Ide, *Spectrochim. Acta*, 2003, **A59**, 1255–98.
- Y. D. Park, T. R. Rizzo, L. A. Peteanu and D. H. Levy, *J. Chem. Phys.*, 1986, **84**, 6539–6549.
- J. R. Carney and T. S. Zwier, *J. Phys. Chem. A*, 2000, **104**, 8677.
- L. Pei, J. Zhang, C. Wu and W. Kong, *J. Chem. Phys.*, 2006, **125**, 024305-1–024305-8.
- L. A. Philips and D. H. Levy, *J. Chem. Phys.*, 1988, **89**, 85–90.
- Y. R. Wu and D. H. Levy, *J. Chem. Phys.*, 1989, **91**, 5278–5284.
- T. Nguyen, T. Korter and D. Pratt, *Mol. Phys.*, 2005, **103**, 1603–1613.
- M. Schmitt, M. Böhm, C. Ratzner, C. Vu, I. Kalkman and W. L. Meerts, *J. Am. Chem. Soc.*, 2005, **127**, 10356–10364.

- 
- 10 T. Nguyen and D. Pratt, *J. Chem. Phys.*, 2006, **124**, 054317-1–054317-6.
  - 11 W. Caminati, *Phys. Chem. Chem. Phys.*, 2004, **6**, 2806–2809.
  - 12 J. R. Clarkson, B. C. Dian, L. Moriggi, A. DeFusco, V. McCarthy, K. D. Jordan and T. S. Zwier, *J. Chem. Phys.*, 2005, **122**, 214311-1–214311-15.
  - 13 B. C. Dian, J. Clarkson and T. S. Zwier, *Science*, 2004, **303**, 1169–1173.
  - 14 M. Schmitt, R. Brause, C. Marian, S. Salzmann and W. L. Meerts, *J. Chem. Phys.*, 2006, **125**, 124309-1–124309-10.
  - 15 T. A. LeGreve, E. E. Baquero and T. S. Zwier, *J. Am. Chem. Soc.*, 2007, **129**, 4028–4038.
  - 16 G. M. Florio, R. A. Christie, K. D. Jordan and T. S. Zwier, *J. Am. Chem. Soc.*, 2002, **124**, 10236–10247.
  - 17 M. Schmitt, J. Küpper, D. Spangenberg and A. Westphal, *Chem. Phys.*, 2000, **254**, 349–361.
  - 18 S. Gerstenkorn and P. Luc, *Atlas Du Spectre D'absorption De La Molécule D'iode*, CNRS, Paris, 1982.
  - 19 S. Wiedemann, A. Metsala, D. Nolting and R. Weinkauff, *Phys. Chem. Chem. Phys.*, 2004, **6**, 2641–2649.
  - 20 R. Ahlrichs, M. Bär, M. Häser, H. Horn and C. Kölmel, *Chem. Phys. Lett.*, 1989, **162**, 165–169.
  - 21 A. Schäfer, C. Huber and R. Ahlrichs, *J. Chem. Phys.*, 1994, **100**, 5829–5835.
  - 22 A. D. Becke, *J. Chem. Phys.*, 1993, **98**, 5648–5652.
  - 23 S. Grimme, *J. Comput. Chem.*, 2007, **25**, 1463–1473.
  - 24 S. Grimme, *J. Comput. Chem.*, 2006, **27**, 1787–1799.
  - 25 H. Horn, H. Weiss, M. Häser, M. Ehrig and R. Ahlrichs, *J. Comput. Chem.*, 1991, **12**, 1058.
  - 26 P. Deglmann, F. Furche and R. Ahlrichs, *Chem. Phys. Lett.*, 2002, **362**, 511–518.
  - 27 A. Ostenmeier, A. Gawelcyk and N. Hansen, in *Parallel Problem Solving from Nature, PPSN III*, ed. Y. Davidor, H.-P. Schwefel and R. Männer, Springer, Berlin/Heidelberg, 1994.
  - 28 I. Kalkman, C. Vu, M. Schmitt and W. L. Meerts, *ChemPhysChem*, 2008, **9**, 1788–1797.
  - 29 J. A. Hageman, R. Wehrens, R. de Gelder, W. L. Meerts and L. M. C. Buydens, *J. Chem. Phys.*, 2000, **113**, 7955–7962.
  - 30 W. L. Meerts, M. Schmitt and G. Groenenboom, *Can. J. Chem.*, 2004, **82**, 804–819.
  - 31 W. L. Meerts and M. Schmitt, *Phys. Scr.*, 2005, **73**, C47–C52.
  - 32 W. L. Meerts and M. Schmitt, *Int. Rev. Phys. Chem.*, 2006, **25**, 353–406.
  - 33 Y. Svartsov and M. Schmitt, in preparation, 2009.
  - 34 Y. K. Sturdy and D. C. Clary, *Phys. Chem. Chem. Phys.*, 2007, **9**, 2065–2074.
  - 35 T. van Mourik and L. E. V. Emson, *Phys. Chem. Chem. Phys.*, 2002, **4**, 5863–5871.
  - 36 G. Varsanyi, *Assignments for Vibrational Spectra of 700 Benzene Derivatives*, Wiley, New York, 1974.
  - 37 M. Schmitt, K. Feng, M. Böhm and K. Kleinermanns, *J. Chem. Phys.*, 2006, **125**, 144303-1–144303-9.
  - 38 L. A. Peteanu and D. H. Levy, *J. Chem. Phys.*, 1988, **92**, 6554–6561.
  - 39 J. R. Carney and T. S. Zwier, *J. Phys. Chem. A*, 1999, **103**, 9943–9957.
  - 40 C. Ratzner, J. Küpper, D. Spangenberg and M. Schmitt, *Chem. Phys.*, 2002, **283**, 153–169.
  - 41 M. Schmitt, D. Krügler, M. Böhm, C. Ratzner, V. Bednarska, I. Kalkman and W. L. Meerts, *Phys. Chem. Chem. Phys.*, 2006, **8**, 228–235.
  - 42 B. Albinsson and B. Nordén, *J. Phys. Chem.*, 1992, **96**, 6204.